ACS APPLIED MATERIALS & INTERFACES

Research Article

www.acsami.org

Synergistic Effects of Morphological Control and Complementary Absorption in Efficient All-Small-Molecule Ternary-Blend Solar Cells

Mahmoud E. Farahat,[†,‡,§] Dhananjaya Patra,[§] Chih-Hao Lee,[†] and Chih-Wei Chu*[,§]

[†]Department of Engineering and System Science, National Tsing-Hua University, Hsinchu 30013, Taiwan, Republic of China

[‡]Nanoscience and Technology Program, Taiwan International Graduate Program, Academia Sinica and National Tsing-Hua University Hsinchu, Taiwan, Republic of China

[§]Research Center for Applied Sciences, Academia Sinica, Taipei 115, Taiwan, Republic of China

Supporting Information

ABSTRACT: In this study, we combined two small-molecule donors—a diketopyrrolopyrrole-based small molecule (SMD) and a benzodithiophene-based molecule (BDT6T)—with [6,6]-phenyl-C_{61}-butyric acid methyl ester ($PC_{61}BM$) to form ternary blend solar cells. The power conversion efficiency of the binary SMD:$PC_{61}BM$ bulk heterojunction solar cell improved from 4.57 to 6.28% after adding an appropriate amount BDT6T as a guest. We attribute this 37% improvement in device performance to the complementary absorption behavior of BDT6T and SMD, as evidenced by the increase in the short circuit current. After addition of BDT6T to form the ternary blend, the crystallinity and morphology of the active layer were enhanced. For example, the features observed in the ternary active layers were finer than those in the binary blends. This means that BDT6T as a third component in the ternary blend has effective role on both the absorption and the morphology. In addition, adding BDT6T to form the ternary blend also led to an increase in the open-circuit voltage. Our findings suggest that the preparation of such simple all-small-molecule ternary blends can be an effective means of improving the efficiency of photovoltaic devices.

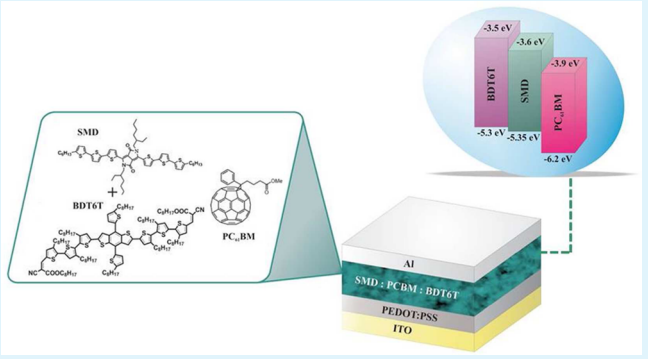

KEYWORDS: *ternary solar cells, small molecules, organic photovoltaics, morphology, bulk heterojunction*

INTRODUCTION

Bulk heterojunction (BHJ) organic photovoltaics (OPVs) are attractive for the production of electricity from solar energy because of their flexibility, lightweight, and simple processability over large areas at low cost. These features, together with the sun as a sustainable source of clean energy, make OPVs among the most promising devices for future energy needs.[1,2] Typically, an OPV employs two organic semiconductors—one a donor (polymer or small molecule) and the other an acceptor (fullerene derivative)—that form what is known as a binary BHJ blend system. The fundamental aspect of a BHJ organic solar cell is its interconnecting bicontinuous nanomorphology.[3] Small molecules have many advantages over their polymeric counterparts, including high charge carrier mobilities, higher crystallinity, and less batch-to-batch variation.[4,5] Single-junction polymer solar cells have achieved power conversion efficiencies (PCEs) of up to 10%,[6] as have single-junction small-molecule solar cells.[7] In a binary BHJ solar cell, the short-circuit current density (J_{sc}) is related mainly to the photoactive layer's absorption profile, which is limited generally by the band gap of the donor material. For that reason, and based on an understanding of the structure−property relationships of the organic donors, several new small molecules have been synthesized to broaden the absorption spectrum. This task can be difficult because the organic donors often have intrinsically narrow absorption widths. As a result, light harvesting in binary organic solar cells is typically poorer than that in devices based on efficient inorganic counterparts. Accordingly, the highest PCE of a single-junction binary organic solar cell has been limited to ∼10%.[8]

Several strategies have been employed to expand the spectral absorption range of organic active layers. For example, donors with different band gaps and absorption behavior can be coupled into tandem-architecture cells. The fabrication of tandem-architecture cells is, however, challenging because several parameters must be controlled, including the active layer thickness in each subcell, the need for a robust intermediate layer for efficient recombination, and the coupling of complementary light absorption between the subcells.[9,10] Ternary blend systems are also promising alternatives. They combine the simplicity of fabricating single-junction active layers with the broader absorption of tandem architectures.[11] In

Received: July 28, 2015
Accepted: September 21, 2015
Published: September 21, 2015

DOI: 10.1021/acsami.5b06831
ACS Appl. Mater. Interfaces 2015, 7, 22542−22550

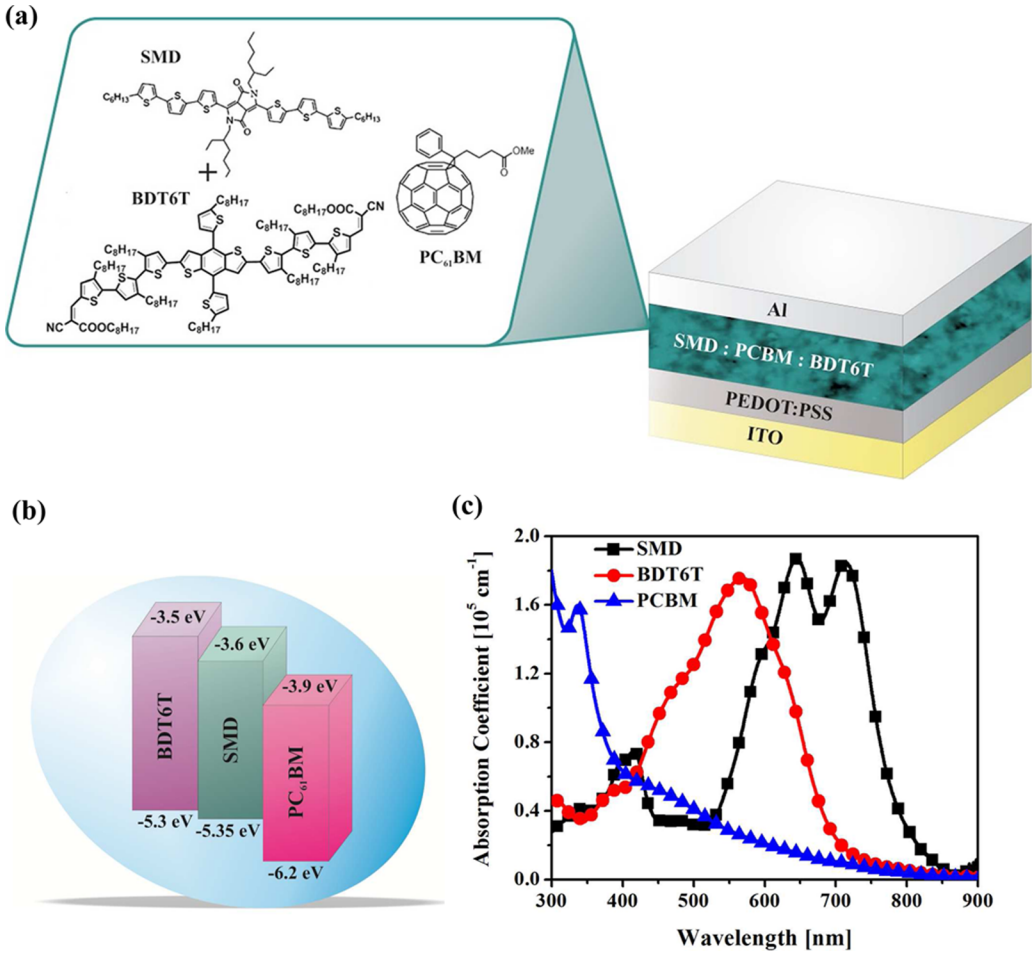

Figure 1. (a) Chemical structures of SMD, BDT6T, and PCBM. (b) Energy levels of SMD, BDT6T, and PCBM. (c) UV−vis absorption spectra of neat SMD, BDT6T, and PCBM thin films.

addition, ternary blends have a great variety of materials from which to form the ternary active layer.[12−14] Successful ternary blends have been formed from two polymer donors and a fullerene acceptor,[15−17] one polymer donor and two fullerene acceptors,[18−21] and a polymer donor, a fullerene acceptor, and a small molecule.[22,23] Mixing two small-molecule donors and a fullerene acceptor to form all-small-molecule ternary devices, the topic of this study, has been reported previously to form a solar cell having a PCE of 1.70%.[24]

The enhancements in PCE of ternary OPV devices can be attributed mainly to the higher values of J_{sc} arising from their broader spectral responses.[11] Nevertheless, tunable open-circuit voltages (V_{oc}) are also possible depending on the composition of the ternary blend; thus, the value of V_{oc} can also be enhanced in a ternary OPV device and not be pinned to the lowest value dictated by the energy levels of its donor and acceptor units.[25,26] Combining the enhancement in J_{sc} with the enhancement in V_{oc} can lead to reasonably high PCEs. Optimization of the morphology of the active layer is another critical parameter, because a nonideal nanomorphology can result in strong bimolecular recombination. Adding a third material to enhance the morphology of the active layer can be an effective approach for controlling the morphology and, thereby, enhancing device performance.[27−33]

Herein, we report an efficient all-small-molecule ternary BHJ solar cell featuring (2*Z*,2′*E*)-dioctyl 3,3′-(5″,5‴′-(4,8-bis(5-octylthiophen-2-yl)benzo[1,2-b:5,4-b′]dithiophene-2,6-diyl)bis-(3,4′,4″-trioctyl-[2,2′: 5′,2′-terthiophene]-5″,5 diyl))bis(2-cyanoacrylate) (BDT6T), a benzodithiophene-based small molecule, as the guest donor in a binary system of a diketopyrrolopyrrole-based small molecule 2,5-di-2-ethylhexyl-3,6-bis-5″-*n*-hexyl-2,2′,5′,2″-terthiophen-5-yl-pyrrolo[3,4-*c*]-pyrrole-1,4-dione (SMD) and [6,6]-phenyl-C_{61}-butyric acid methyl ester ($PC_{61}BM$). Relative to the binary SMD:$PC_{61}BM$ system, the ternary blend system exhibited simultaneous enhancements in the values of J_{sc}, V_{oc}, and the fill factor (FF), leading to a PCE of 6.3% (a 37% improvement over that provided by the binary blend) under optimized conditions. We attribute this enhanced performance in part to the increase in J_{sc} arising from the complementary absorption behavior of BDT6T and SMD. In addition, the crystallinity and morphology of the active layer were enhanced after the addition of BDT6T to form the ternary blend. For example, features in the ternary active layers were finer than those in the binary blend. Adding BDT6T to form the ternary blend also increased the value of V_{oc}, suggesting the formation of an organic alloy with energy levels for the highest occupied molecular orbital (HOMO) and lowest unoccupied molecular orbital (LUMO) that were based on their average composition. In addition to measurements of device performance, we also studied this ternary blend system using UV−vis absorption spectroscopy, atomic force microscopy (AFM), grazing incidence X-ray diffraction (GIXD), photoluminescence (PL), and measurements of external quantum efficiency (EQE).

DOI: 10.1021/acsami.5b06831
ACS Appl. Mater. Interfaces 2015, 7, 22542−22550

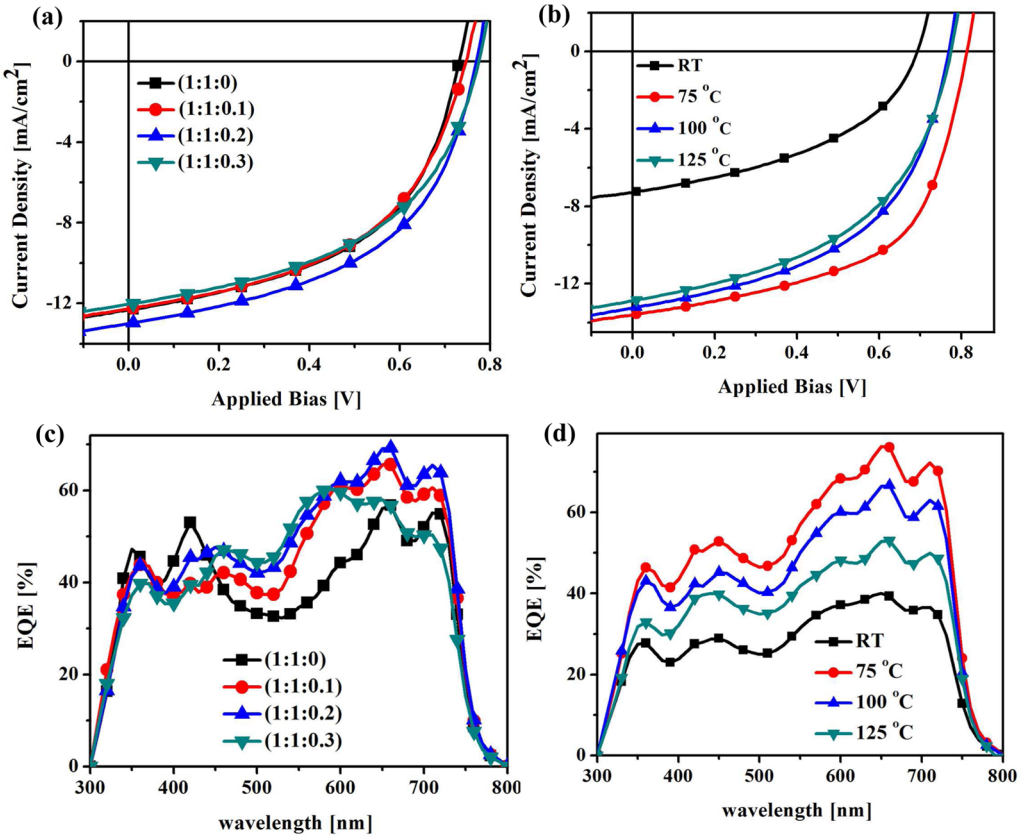

Figure 2. (a, b) *J*−*V* photovoltaic characteristic of (a) devices based on the SMD:PCBM:BDT6T ternary blend (1:1:*X*), where *X* is 0, 0.1, 0.2, and 0.3 (devices postannealed at 100 °C) and (b) devices based on the SMD:PCBM:BDT6T ternary blend (1:1:0.2) that had been subjected to postannealing at various temperatures. (c, d) Corresponding EQE spectra.

EXPERIMENTAL SECTION

Materials and Solutions Preparation. The dialkylated diketopyrrolopyrrole chromophore SMD (purity > 99%) was obtained from Luminescence Technology (Lumtec). $PC_{61}BM$ was purchased from Solenne b.v. The conducting polymer poly(3,4-ethylenedioxythiophene)/polystyrenesulfonate (PEDOT:PSS) was obtained from Clevios (PVP 4083). The solvent additive (3-chloropropyl)-trimethoxysilane (CP3MS) was purchased from Alfa Aesar. Small molecule donor BDT6T was prepared earlier by our group.[34] A solution of SMD and $PC_{61}BM$ in 0.1% CP3MS-containing chlorobenzene was heated at 70 °C in a glovebox. To form ternary blends, different amounts of BDT6T were added to form ratios of SMD/PCBM/BDT6T of 1:1:*X*, where *X* ranged from 0.1 to 0.3 in weight.

Device Fabrication. Devices were fabricated on 0.1 cm^2 prepatterned indium tin oxide (ITO)-coated glass substrates (sheet resistance: 15 Ω square^{-1}) with the conventional device structure ITO/PEDOT:PSS (40 nm)/SMD:$PC_{61}BM$:BDT6T blend [1:1:*X* (w/w); donor concentration of 10 mg mL^{-1}]/Al (100 nm). Prior to device fabrication, the ITO-coated glass substrates were cleaned using standard procedures, including sonication in detergent followed by rinsing in deionized water, and then treated with UV/ozone for 15 min. The solution of PEDOT:PSS was passed through a 0.45 mm syringe filter onto the clean substrates, which were then spin-coated (4000 rpm) and annealed in air for 30 min at 130 °C. The active layer was then spin-coated at various speeds for 60 s inside a glovebox filled with N_2. The optimum active layer thickness is 100 nm. Finally, the Al cathode (100 nm) was deposited through thermal evaporation in a vacuum chamber (7 × 10^{-6} Torr). Postannealing (annealing the full device after Al electrode deposition) of the devices was performed at various temperatures (75, 100, 125 °C) inside a glovebox filled with N_2. The configurations of the hole-only and electron-only devices were ITO/PEDOT:PSS/small molecule:$PC_{61}BM$/V_2O_5/Al and ITO/Cs_2CO_3/small molecule:$PC_{61}BM$/Ca/Al, respectively. The electron and hole motilities were determined by fitting the plots of the dark *J*−*V* curves for single-carrier devices to the SCLC model.[35]

Device Characterization. Absorption spectra of the films were measured using a Jacobs V670 UV−vis−NIR spectrophotometer. The photovoltaic performance of each device was measured inside a glovebox filled with N_2 under simulated AM 1.5 G illumination (100 W cm^{-2}) using a Xe lamp-based solar simulator (Thermal Oriel 1000 W). The light intensity was calibrated using a monosilicon photodiode featuring a KG-5 color filter (Hamamatsu). EQE spectra were recorded using a QE-R apparatus (Enlitech) operated in AC mode. The devices were encapsulated within a glovebox filled with N_2 prior to removal for the EQE measurements. A Bruker Innova atomic force microscope (Digital Instrument NS 3a controller equipped with a D3100 stage) was used, in the tapping mode, to record the surface morphologies of the active layers. XRD experiments were performed using X-rays having a wavelength of 1.0252 Å at the superconducting wiggler beamline BL13A1 of the National Synchrotron Radiation Research Center, Taiwan. PL spectra were recorded using a fluorescence spectrophotometer (F-4500, Hitachi, Tokyo, Japan) with a Xe lamp operated at 150 W as the excitation source at an excitation wavelength of 405 nm.

RESULTS AND DISCUSSION

Figure 1a,b presents the chemical structures and energy levels, respectively, of the materials used in this study. SMD is the host donor, and $PC_{61}BM$ is the acceptor. BDT6T is used as a third component (guest donor) to form the ternary blend. The HOMO levels of SMD and BDT6T are 5.35 and 5.3 eV respectively, while LUMO levels of SMD and BDT6T have been also reported to be 3.6 and 3.5 eV, respectively.[19,36] BDT6T was added at various amounts to the SMD:$PC_{61}BM$

DOI: 10.1021/acsami.5b06831
ACS Appl. Mater. Interfaces 2015, 7, 22542−22550

Table 1. Photovoltaic Characteristics of Ternary Blend Devices Prepared Using Different Amounts of BDT6T and Different Post-Annealing Temperatures[a]

SMD:PCBM:BDT6T	post. ann. temp [°C]	J_{sc} [mA cm^{-2}]	V_{oc} [V]	FF [%]	PCE [%]	R_s [Ω·cm^2]
1:1:0	100	12.31	0.73	50.86	4.57	2.53
1:1:0.1	100	12.26	0.75	49.05	4.51	3.23
1:1:0.2	100	13.00	0.77	50.59	5.06	1.90
1:1:0.3	100	12.04	0.78	48.34	4.54	3.35
1:1:0.2	RT	7.27	0.69	43.86	2.20	15.56
1:1:0.2	75	13.61	0.81	56.97	6.28	1.86
1:1:0.2	100	13.22	0.77	50.69	5.16	2.03
1:1:0.2	125	12.88	0.77	48.28	4.85	4.98

[a]All devices were cast from chlorobenzene containing 0.1% CP3MS as a solvent additive. RT = room temperature.

binary blend. Herein, we refer to the SMD:PCBM:BDT6T ternary blends in terms of their blend ratios (1:1:*X*). All solutions were prepared in chlorobenzene containing 0.1% CP3MS, following the approach we described in a previous report.[37] CP3MS as solvent additive was reported to have positive effect on the morphology of SMD:PCBM binary system, which can be noticed in PCE enhancement. Figure 1c displays the absorption spectra of neat SMD, BDT6T, and PCBM. All of these films were annealed at 75 °C for 10 min inside a glovebox filled with N_2. The spectrum of the neat SMD film features a broad absorption over the entire visible spectrum up to 800 nm, with four absorption peaks. The high-energy absorption band at 416 nm represents the $\pi-\pi^*$ transitions in both the diketopyrrolopyrrole (DPP) core and thiophene units. For wavelengths in the region of 500−800 nm, three absorption peaks are evident: at 594, 644, and 714 nm. We attribute the former two to intramolecular charge transfer between the DPP and oligothiophene units and the latter to transitions involving an aggregate species arising from strong intermolecular interactions.[36] The spectrum of pure BDT6T features absorptions in the range from 400 to 700 nm with a maximum at 565 nm, complementing the absorption spectrum of SMD. When combined with PCBM, the three components in the single-junction active layer covered absorption spectrum from 300 to 800 nm.

We investigated the photovoltaic characteristics of SMD:PCBM:BDT6T ternary blends prepared under different fabrication conditions. In a previous study, we found that the SMD:PCBM binary system provided a device exhibiting a PCE of 4.55% when we prepared the active layer using CP3MS as a solvent additive in conjunction with postannealing treatment.[37] We ascribed the enhancement in PCE to the improvements in both the value of J_{sc} and the FF. For the SMD:PCBM binary system postannealed at 100 °C for 10 min (no CP3MS additive used), the PCE reached 3.5%. In this present study, we initially examined the addition of BDT6T to form the ternary blend having a blend ratio of (1:1:0.2). When we postannealed this ternary active layer at 100 °C for 10 min (no CP3MS additive used), we obtained a significant improvement in PCE (Figure S1 and Table S1 in the Supporting Information)—from 3.5% for the binary blend to 4.7% for the ternary blend—with simultaneous enhancements in the values of J_{sc}, V_{oc}, and the FF. These promising results suggested that further improvements might be possible when using CP3MS as an additive.

Figure 2a and Table 1 display the effect of adding BDT6T into the binary blend to form SMD:PCBM:BDT6T ternary blend systems at various ratios (1:1:*X*), where *X* was 0.1, 0.2, or 0.3 in weight. These ternary active layers were cast from chlorobenzene containing 0.1% CP3MS as a solvent additive and then postannealed at 100 °C for 10 min. The optimal ternary blend ratio, where the values of J_{sc} and V_{oc} were enhanced significantly relative to those of the binary system, was 1:1:0.2, and the PCE increased to 5.06% from a value of 4.57% for the binary blend system. One possible reason for the increase in the value of J_{sc} is the complementary absorption behavior of BDT6T, which complements the missing part absorption of SMD at wavelengths between 400 to 600 nm.

Interestingly, increasing the BDT6T ratio in the blend caused the value of V_{oc} to increase. For the device prepared from the SMD:PCBM binary blend system, we obtained a value of V_{oc} of 0.73 V (Table 1), consistent with literature reports.[37,38] Device performance of the binary BDT6T:PCBM blend system is shown in Figure S2 and Table S2, which is consistent with a previous study where V_{oc} has value of 0.90 V.[34] For the ternary blend systems, the value of V_{oc} reached its maximum of 0.78 V at a blend ratio of 1:1:0.3. The open-circuit voltage is primarily determined by the difference between the HOMO energy level of the donor and the LUMO energy level of the acceptor. The energy level diagram in Figure 1b shows HOMO levels of SMD and BDT6T of 5.35 and 5.3 eV, respectively. With the LUMO energy level of PCBM being ∼3.9 eV, an interface gap of 1.4 eV exists. Another interface gap of 1.6 eV also exists between the HOMO of BDT6T and the LUMO of SMD. A wider energy difference between the LUMO of the acceptor and the HOMO of the donor at the BDT6T−SMD, BDT6T−PCBM, and SMD−PCBM junctions would lead to an elevated open-circuit voltage. Thompson[39] revealed that the D/D and A/A components in ternary donor/donor/acceptor (D/D/A) and donor/acceptor/acceptor (D/A/A) composites, respectively, form organic alloys featuring HOMO and LUMO energy levels based on their average composition.[25,40] Therefore, the charge transfer state energy and, consequently, the value of V_{oc} of the ternary blend changes as the ratio of either the donors or acceptors is changed. This phenomenon allows higher values of V_{oc} in ternary D/D/A systems than are possible in binary D/A systems. Thus, we conclude that the increases in the open-circuit voltages in our ternary blends arose from improved alignment of the energy levels between the frontier molecular orbitals at the D/A and D/D interfaces. The FFs obtained under these fabrication conditions changed slightly relative to those of the binary blend system [Figure 2a]. Ultimately, the PCE enhanced to 5.06% at a ternary blend ratio of 1:1:0.2, compared with a value of 4.57% for the binary blend system.

For further optimization of the system at a ternary ratio of 1:1:0.2, we examined the effect of the postannealing temperature (75, 100, or 125 °C). Figure 2b and Table 1 display the photovoltaic characteristics of devices prepared using the different postannealing conditions. Compared with the

DOI: 10.1021/acsami.5b06831
ACS Appl. Mater. Interfaces 2015, 7, 22542−22550

performances of the devices prepared without postannealing, we observed significant enhancements in all of the device parameters (J_{sc}, V_{oc}, FF) at all annealing temperatures. The significant effects of postannealing on device performance have been reported previously.[41,42] Employing the optimized blend ratio, the ternary SMD:PCBM:BDT6T system (1:1:0.2) provided its best device performance when the postannealing temperature was 75 °C, achieving a PCE of 6.28% with a value of J_{sc} of 13.61 mA cm^{-2}, a value of V_{oc} of 0.81 V, and an FF of 57%.

Figure 2c displays the EQE measurements of devices featuring different amounts of BDT6T added to the SMD:PCBM blend. Previous studies of the EQE spectra of ternary blends have revealed either local enhancements corresponding to the absorption of the guest material or overall enhancements over the entire range of wavelengths.[16,43] In this present study, we observed that the incorporation of BDT6T into the SMD:PCBM blend increased the EQEs over the region corresponding to the absorption of BDT6T (450–650 nm). In addition, we noted improvements in the SMD absorption region from 600 to 800 nm for the ternary blends at ratios of 1:1:0.1 and 1:1:0.2, which is mainly attributed to the enhanced SMD crystallinity. Thus, BDT6T effectively contributed to the light harvesting of SMD to cover wavelengths over the range from 300 to 800 nm. Increasing the amount of BDT6T in the ternary blend significantly increased the amount of light harvested up to a ternary blend ratio of 1:1:0.2, as indicated in the EQE spectra. Further increasing the amount of BDT6T in the ternary blend decreased in the EQE, especially in the absorption range of SMD. The addition of BDT6T at the optimal ratio (1:1:0.2) achieved an EQE of 69%, compared with a value of 56% for the binary SMD:PCBM blend. Figure 2d displays the EQEs obtained for the optimal ternary blend ratio of 1:1:0.2 after postannealing at various temperatures. It confirms that one reason for the enhanced values of J_{sc} after the addition of BDT6T was the greater light-harvesting ability of the ternary blend. The enhanced EQE arising from the contributions of both SMD and BDT6T in the ternary blend can also be ascribed to the change in film composition. We can approximately quantify the enhancement in the PCE that resulted from enhanced light harvesting compared to the improved morphology due to BDT6T addition. At 1:1:0.2 ternary blend ratio, the EQE enhancement in the range of ~700 nm is mainly attributed to the enhanced morphology. Compared to the binary blends, the EQE enhancement resulting from morphology change due to BDT6T addition might be more than 50% of the full enhancement. Figure S3 in the Supporting Information shows the internal quantum efficiency (IQE) of devices with different amounts of BDT6T added to the SMD:PCBM blend consistent with EQE.

The absorption spectra of blend films can provide information regarding the molecular ordering of their components. Figure 3a displays the effect of adding different amounts of the small molecule BDT6T to the binary SMD:PCBM blend. All of these films had been annealed at 75 °C for 10 min inside a glovebox filled with N_2. In the absence of BDT6T, mixing SMD with PCBM led to a slight blue shift in the aggregate absorption band relative to that for neat SMD (from 714 to 707 nm). Furthermore, the intensity of this aggregate peak for neat SMD decreased after mixing with PCBM, indicative of disruption of the donor packing after the addition of fullerene molecules.[38,44] Adding BDT6T to form ternary blends led to significant enhancements in the peak

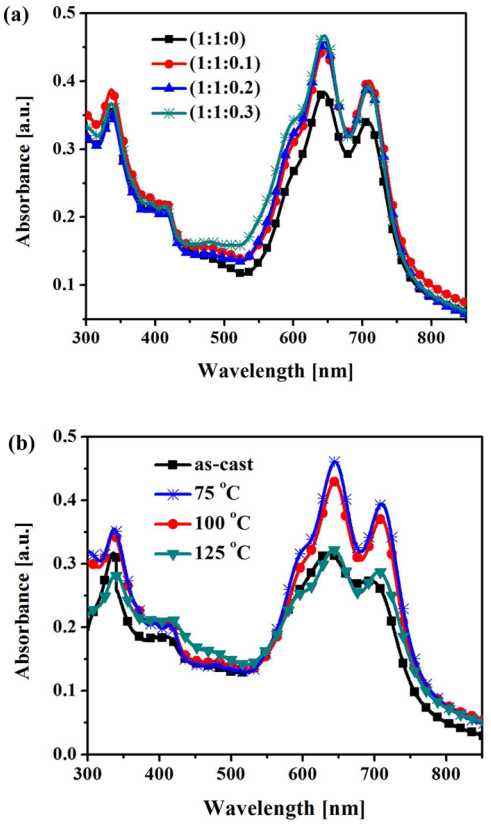

Figure 3. UV–vis absorption spectra displaying the effects on the absorptions of ternary blends after (a) adding BDT6T and (b) applying different annealing temperatures.

intensities over the whole absorption spectrum. For the 1:1:0.1 ternary blend, we attribute the enhancement in the wavelength region of 400–600 nm mainly to the complementary absorption effect of the addition of BDT6T as a guest donor. Interestingly, we observed clear enhancements in the main absorption peaks of SMD at 594, 644, and 707 nm relative to those of the active layers prepared without BDT6T, presumably because of increased molecular ordering of the SMD donor molecules after the addition of BDT6T. Increasing the amount of BDT6T in the ternary blend increased the intensity of the signals from SMD, suggesting that BDT6T induced the crystallization of SMD. Although the absorption signals at 594, 644, and 707 nm become more prominent upon increasing the content of BDT6T, increasing the amount of BDT6T beyond 0.3 (w/w) slightly suppressed the peak at 707 nm, but it remained more intense than that from thin films prepared without BDT6T. This behavior suggests that well-ordered SMD molecules formed through aggregation and crystallization, due to intramolecular interactions with BDT6T. Therefore, we suspect that the optimal amount of BDT6T facilitated the crystallization of SMD in the ternary blend system.

Figure 3b displays the UV–vis spectra of active layers cast from the ternary blend at a ratio of 1:1:0.2 that had been subjected to annealing at temperatures of 75, 100, and 125 °C. Upon increasing the annealing temperature, the vibronic peaks of SMD become more prominent compared with those from the nonannealed active layer, indicating a higher degree of ordering in the donor phase.[44] The annealing temperature that provided the most significant vibronic features was 75 °C. Increasing or decreasing the annealing temperature from 75 °C

DOI: 10.1021/acsami.5b06831
ACS Appl. Mater. Interfaces 2015, 7, 22542–22550

dramatically affected the film's crystallinity. Increasing the amount of BDT6T had an effect on the crystallinity of films (vibronic peaks) cast from the ternary blends that was similar to that of increasing the annealing temperature. Both had optimal conditions at which the molecular ordering of SMD was the highest. By analogy, we can conclude that BDT6T acted as a crystallizing agent in the ternary blend and successfully modulated the crystallization of SMD domains. Thus, BDT6T played two roles in the ternary blends: as a complementary absorption component and as a crystallizing agent. It is well-established that[44] the value of J_{sc} depends strongly on the absorption intensity, derived from the crystallinity, of the donor. The effect of BDT6T on the crystallinity of SMD was clear from the UV−vis absorption spectra in Figure 3. Accordingly, the enhanced crystallinity of SMD induced upon the addition of BDT6T might be another reason for the enhanced values of J_{sc}. Combining these observations with the device performance data, we can confirm that BDT6T had a positive influence on not only the light-harvesting capability but also the morphology and crystallinity of the SMD domains in the ternary active layer.

We recorded PL spectra to examine the kinetic processes of energy transfer and charge carrier transport in the ternary blend films. Figure 4a presents the PL spectra of neat SMD and BDT6T and of binary blend active layers of SMD:PCBM, BDT6T:PCBM, and SMD:BDT6T under excitation at 405 nm. The PL emission peaks appear at 750 and 825 nm for neat SMD and at 724 nm for neat BDT6T. Because these PL emissions of SMD and BDT6T overlap, Förster energy transfer is energetically favorable at the BDT6T−SMD interface. Excitons generated in BDT6T diffuse efficiently to SMD prior to diffusion to an interface with PCBM for dissociation.[45] The PL emissions of the pristine SMD and BDT6T films were quenched significantly upon blending with PCBM. The same significant quenching was noticed in the binary blend system of BDT6T:PCBM. This highly efficient PL quenching might be ascribed to the possible charge transfer pathway between SMD:PCBM, BDT6T:PCBM, and SMD:BDT6T as well. For the binary SMD and PCBM blend, the emission from SMD was quenched primarily by PCBM. Adding BDT6T with different ratios to form the ternary system caused the emission from SMD in the SMD:PCBM mixture to become further quenched as shown in Figure 4b. This observation suggests that almost all the BDT6T excitons were efficiently transferred to SMD molecules, confirming the existence of energy transfer from BDT6T to SMD.[8,46] The quenching in the ternary blends at ratios of 1:1:0.2 and 1:1:0.3 was higher than that in the binary system and 1:1:0.1 ternary blend. From these observations, we conclude that incorporation of BDT6T decreased the PL of the blend, suggesting that fewer excitons were quenched through radiative recombination, leading to higher exciton diffusion efficiency.[47] Thus, we can attribute the higher values of J_{sc} and FF observed after the addition of BDT6T not only to its contribution to light harvesting but also to efficient exciton diffusion. The energy transfer between SMD and BDT6T was also confirmed by the $J-V$ photovoltaic characteristic of SMD:BDT6T shown in Figure S4 and Table S3. Clearly, the blends of SMD:BDT6T also exhibit a photoresponse, due to the ambipolarity of BDT6T. Even though its photocurrent is low compared to binary or ternary devices, the ambipolarity of BDT6T makes it possible to prepare multijunctions, thereby increasing the interface for charge separation, leading to greater photocurrents when mixed in the ternary blend.

We recorded AFM images (tapping mode) to further investigate the effect of BDT6T on the morphologies of the ternary active layers at various blend ratios. The binary active layer of SMD:PCBM [Figure 5a] featured an inhomogeneous distribution of large SMD domains. Adding BDT6T had a significant influence on the morphology of the ternary active

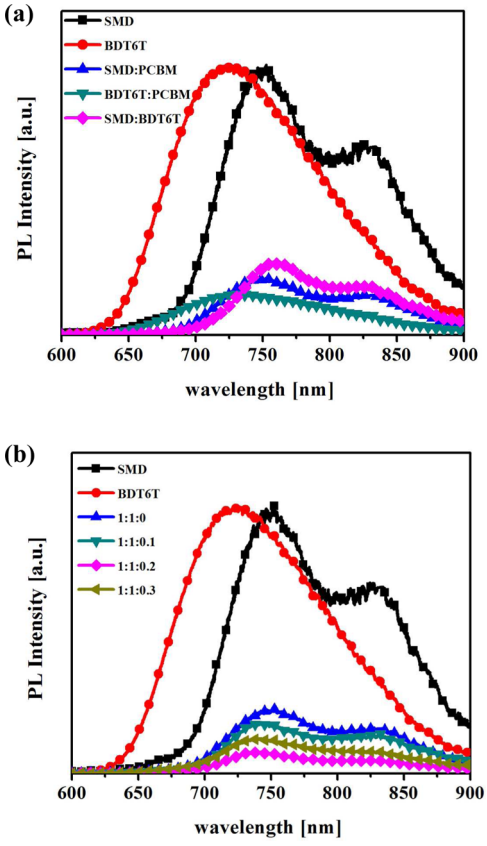

Figure 4. PL spectra of (a) the neat donors and of active layers based on binary blends and (b) for SMD:PCBM:BDT6T ternary blends (1:1:X), where X = 0, 0.1, 0.2, and 0.3.

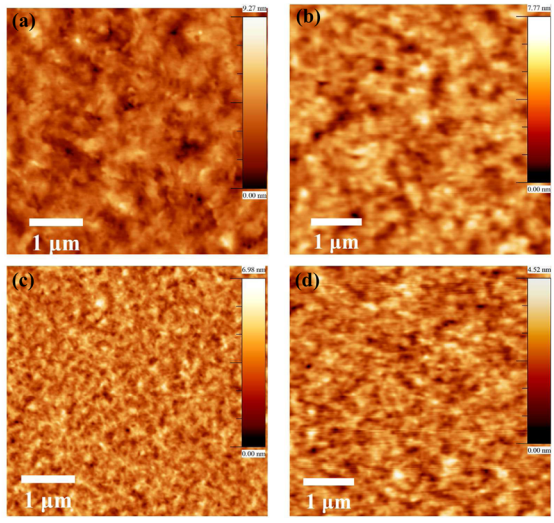

Figure 5. AFM height images of active layers based on SMD:PCBM:BDT6T ternary blends 1:1:X. (a) X = 0, (b) X = 0.1, (c) X = 0.2, and (d) X = 0.3.

DOI: 10.1021/acsami.5b06831
ACS Appl. Mater. Interfaces 2015, 7, 22542−22550

layers. The ternary blend of 1:1:0.1 [Figure 5b] possessed smaller, well-distributed SMD domains. Increasing the amount of BDT6T in the ternary blend to 1:1:0.2 gave an active layer [Figure 5c] exhibiting finer features relative to those in the 1:1:0.1 ternary blend. Further increasing the ratio of BDT6T in the blend to 1:1:0.3 [Figure 5d] led to an increase in the domain size relative to that of the 1:1:0.2 ternary blend, but it remained smaller than that in the binary active layer. Significant differences in the roughnesses of the active layers were evident after incorporation of BDT6T in the blend. The ternary blends at ratios of 1:1:0.1, 1:1:0.2, and 1:1:0.3 had roughnesses (rms) of 1.8, 1.3, and 0.93 nm, respectively, that were lower than that of the binary active layer (2.4 nm). Thus, we conclude that adding BDT6T tailored the morphology of the ternary active layer. BDT6T acted as a refining agent, forming smaller SMD domains with more homogeneous distribution than those formed in the active layer in its absence. Smaller SMD domains with less PCBM agglomeration led to larger interfaces between the donor and acceptor components, as required for better charge dissociation.[31,48] Control over the morphology of the ternary active layer might be another reason, in addition to complementary absorption, for the higher values of J_{sc} obtained for devices containing BDT6T. A thiophene-containing small molecule has been found to act as a nucleating agent to improve the conformation of polymer chains and enhance their crystallinity.[49] Accordingly, we conclude that BDT6T, a small molecule containing thiophene units, could function as a morphology controller, inducing a favorable active layer morphology with interpenetrating nanoscale domains. Figure S5 shows AFM images (tapping mode) with higher resolution for different conditions. Figure S6 and Table S4 show the charge carrier mobility measurements of devices based on SMD:PCBM:BDT6T ternary blends with different BDT6T ratios. On the basis of the fitting of the dark current by the SCLC model, electron and hole mobilities of the 1:1:0 were found to be 5.30×10^{-8} and 8.5×10^{-9} m^2 V^{-1} s^{-1}, respectively, with charge carrier mobility ratio μ_e/μ_h of 6.2. After BDT6T addition to form the ternary blend, the μ_e/μ_h ratio decreased to 1.78, 1.55, and 1.40 for blend ratios of 1:1:0.1, 1:1:0.2, and 1:1:0.3, respectively, exhibited much more balanced charge transport properties. The results indicate that adding BDT6T in the ternary blend is not only beneficial for complementary absorption and morphology control but also enhanced the hole mobility leading to more balanced charge transport.

We used GIXD to further investigate the effect of BDT6T in the ternary blend and its impact on the PCE. Figure 6a presents the GIXD spectra of the neat donors SMD and BDT6T and of their blend. The neat SMD film exhibited a characteristic X-ray reflection at a value of q of 0.446 $Å^{-1}$ (d = 14.08 Å) arising from the lamellar structure of SMD crystallites. The neat BDT6T film exhibited a characteristic X-ray reflection at 0.268 $Å^{-1}$ (d = 23.44 Å) reflecting the lamellar structure of single BDT6T crystals. Blending BDT6T with SMD caused two reflection peaks to appear: one at 0.256 $Å^{-1}$ (d = 24.54 Å) assigned to BDT6T crystallites and the other at 0.437 $Å^{-1}$ (d = 14.38 Å) for SMD crystallites. Although the peak of BDT6T broadened and was less intense than that in its neat state, the SMD peak was only slightly changed relative to that of neat SMD. Figure 6b displays the GIXD patterns of the active layers in the absence of BDT6T (binary) and in its presence (ternary) at various amounts. The pattern of the SMD:PCBM binary blend system featured two peaks: one at 0.211 $Å^{-1}$ (d = 29.78 Å) and another at 0.44 $Å^{-1}$ (d = 14.28 Å). We assign the latter to crystalline, well-ordered SMD and the former to a stacking of layers of SMD. Layers in the stacking structure are separated by the PCBM, which can interfere with the nucleation sites of small-molecule crystallites.[20,38,44] This result is consistent with the absorption spectra in Figure 3a, where the suppression of the peak at 707 nm was due to disruption of donor packing after the addition of the fullerene. In addition, SMD layers are stacked in a random way azimuthally because the shape of the diffraction peak is very asymmetric.[50] The signal for the crystalline, well-ordered SMD at 0.44 $Å^{-1}$ in the blend appeared at a slightly lower value of q relative to that for the neat SMD (q = 0.446 $Å^{-1}$), possibly because PCBM interfered with the SMD molecules. Adding BDT6T to SMD:PCBM to form ternary blend systems resulted in two peaks appearing for all of the examined ratios. For the 1:1:0.1 active layer, the main peak, attributed to crystalline, well-ordered SMD, remained almost unchanged at 0.445 $Å^{-1}$. A significant shift to a higher value of q occurred for the peak corresponding to layer stacking SMD phase (q = 0.26 $Å^{-1}$). This peak underwent further shifting to higher values of q upon increasing the BDT6T content. For the 1:1:0.2 blend, it shifted to 0.3 $Å^{-1}$, while the other peak (for crystalline, well-ordered SMD) remained unchanged at 0.445 $Å^{-1}$. For the 1:1:0.3 blend, the two peaks shifted toward lower slightly values of q: 0.292 $Å^{-1}$ for the stacked layers of SMD phase and 0.436 $Å^{-1}$ for the crystalline, well-ordered SMD. For all of the ternary active layers, significant increase in peak intensity and more narrow diffraction width at 0.445 $Å^{-1}$ occurred after incorporating BDT6T into the ternary blend,

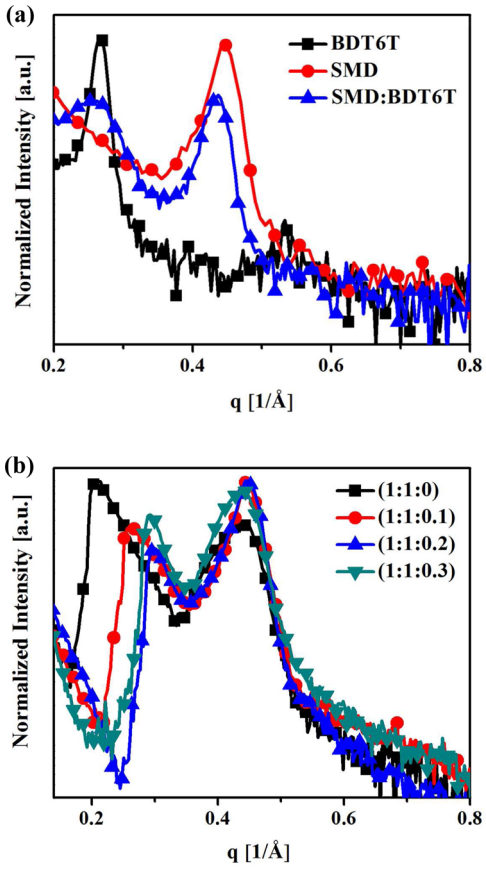

Figure 6. GIXD patterns of (a) neat donors and (b) active layers based on SMD:PCBM:BDT6T ternary blends (1:1:X), where X = 0, 0.1, 0.2, and 0.3.

DOI: 10.1021/acsami.5b06831
ACS Appl. Mater. Interfaces 2015, 7, 22542−22550

an indication of better crystallinity of SMD in the active layer. The increase in the degree of crystallinity might be attributable to the increased content of small-molecule crystals (SMD, BDT6T) dispersed in the blend system, increasing the number of nucleation sites for SMD crystallites, consistent with the AFM images and confirming the refining effect of BDT6T in the ternary blend. Thus, the enhanced values of J_{sc} can be explained by the increased number of nanoscale SMD crystallites leading to larger interfacial areas between the donors and acceptor and, consequently, facilitating charge dissociation and the transport of charge carriers in the active layer. The peak at 0.211 $Å^{-1}$ (d = 29.78 Å) in the binary blend experienced significant shifts toward higher values of q upon increasing the BDT6T content in the ternary blend, reaching values of 0.26 $Å^{-1}$ (d = 24.17 Å) and 0.3 $Å^{-1}$ (d = 20.94 Å) for ternary blend ratios of 1:1:0.1 and 1:1:0.2, respectively, thereafter remaining almost unchanged for the 1:1:0.3 ternary blend ratio (q = 0.292 $Å^{-1}$; d = 21.52 Å). Shifting toward higher values of q implies that the addition of BDT6T induced greater packing and ordering of the layer stacking of SMD phase—further evidence for the role of BDT6T as a crystallizing agent in the ternary blend. The normal XRD patterns in Figure S7 (Supporting Information) reveal a similar trend, confirming the role of BDT6T as a crystallizing agent.

CONCLUSION

We have examined the effects of adding various amounts of BDT6T, a small-molecule donor, to a binary SMD:PCBM blend to form ternary blend systems for use as active layers in BHJ solar cells. The devices incorporating the ternary blends exhibited significantly improved PCEs—reaching 6.3% (a 37% improvement)—relative to that of the binary system. We observed simultaneous enhancements in the values of all the device parameters when using the optimized ternary blend ratio and postannealing temperature. The absorption of BDT6T is complementary to that of SMD, together covering absorption wavelengths from 300 to 800 nm, in part explaining the increase in the values of J_{sc}. In addition, BDT6T enhanced the crystallization of SMD in the active layer and, at the same time, resulted in the formation of finer features that were favorable for charge separation. Adding BDT6T to form the ternary blend also increased the value of V_{oc}, suggesting the formation of an organic alloy with HOMO and LUMO energy levels based on their average composition. This study opens new directions for the design of new ternary structures and the development of high-performance molecular solar cells.

ASSOCIATED CONTENT

Supporting Information

The Supporting Information is available free of charge on the ACS Publications website at DOI: 10.1021/acsami.5b06831.

Photovoltaic characteristics of the condition used to optimize the ternary blend system (ternary blend without additive), SMD:BDT6T, and BDT6T:PCBM. IQE, AFM, mobility measurements, and XRD profiles of active layers of SMD:PCBM:BDT6T at various blend ratios. (PDF)

AUTHOR INFORMATION

Corresponding Author

*Phone: +886-2-2787-3183. Fax: +886-2-2787-3122. E-mail: gchu@gate.sinica.edu.tw.

Notes

The authors declare no competing financial interest.

ACKNOWLEDGMENTS

We thank the Taiwan Ministry of Science and Technology (102−2221−E−001−029−MY2), the Center for Sustainability Science of Academia Sinica, Taiwan (AS−103−SS−A02), and Academia Sinica, Taiwan (Career Development Award 103−CDA−M01) for financial support, and NanoCore, the Core Facilities for Nanoscience and Nanotechnology at Academia Sinica, Taiwan, for technical support.

REFERENCES

(1) Li, G.; Zhu, R.; Yang, Y. Polymer Solar Cells. *Nat. Photonics* **2012**, *6* (3), 153−161.
(2) Cao, W.; Xue, J. Recent Progress in Organic Photovoltaics: Device Architecture and Optical Design. *Energy Environ. Sci.* **2014**, *7* (7), 2123−2144.
(3) Heeger, A. J. 25th Anniversary Article: Bulk Heterojunction Solar Cells: Understanding the Mechanism of Operation. *Adv. Mater.* **2014**, *26* (1), 10−28.
(4) Lin, Y.; Li, Y.; Zhan, X. Small Molecule Semiconductors for High-Efficiency Organic Photovoltaics. *Chem. Soc. Rev.* **2012**, *41* (11), 4245−4272.
(5) Mishra, A.; Bäuerle, P. Small Molecule Organic Semiconductors on the Move: Promises for Future Solar Energy Technology. *Angew. Chem., Int. Ed.* **2012**, *51* (9), 2020−2067.
(6) Chen, J.-D.; Cui, C.; Li, Y.-Q.; Zhou, L.; Ou, Q.-D.; Li, C.; Li, Y.; Tang, J.-X. Single-Junction Polymer Solar Cells Exceeding 10% Power Conversion Efficiency. *Adv. Mater.* **2015**, *27* (6), 1035−1041.
(7) Kan, B.; Zhang, Q.; Li, M.; Wan, X.; Ni, W.; Long, G.; Wang, Y.; Yang, X.; Feng, H.; Chen, Y. Solution-Processed Organic Solar Cells Based on Dialkylthiol-Substituted Benzodithiophene Unit with Efficiency Near 10%. *J. Am. Chem. Soc.* **2014**, *136* (44), 15529−15532.
(8) Yang, L.; Yan, L.; You, W. Organic Solar Cells beyond One Pair of Donor−Acceptor: Ternary Blends and More. *J. Phys. Chem. Lett.* **2013**, *4* (11), 1802−1810.
(9) Ameri, T.; Li, N.; Brabec, C. J. Highly Efficient Organic Tandem Solar Cells: A Follow up Review. *Energy Environ. Sci.* **2013**, *6* (8), 2390−2413.
(10) You, J.; Dou, L.; Hong, Z.; Li, G.; Yang, Y. Recent Trends in Polymer Tandem Solar Cells Research. *Prog. Polym. Sci.* **2013**, *38* (12), 1909−1928.
(11) Ameri, T.; Khoram, P.; Min, J.; Brabec, C. J. Organic Ternary Solar Cells: A Review. *Adv. Mater.* **2013**, *25* (31), 4245−4266.
(12) Lu, L.; Kelly, M. A.; You, W.; Yu, L. Status and Prospects for Ternary Organic Photovoltaics. *Nat. Photonics* **2015**, *9* (8), 491−500.
(13) Goubard, F.; Wantz, G. Ternary Blends for Polymer Bulk Heterojunction Solar Cells. *Polym. Int.* **2014**, *63* (8), 1362−1367.
(14) Cheng, P.; Zhan, X. Versatile Third Components for Efficient and Stable Organic Solar Cells. *Mater. Horiz.* **2015**, *2* (5), 462−485.
(15) Ameri, T.; Heumuller, T.; Min, J.; Li, N.; Matt, G.; Scherf, U.; Brabec, C. J. IR Sensitization of an Indene-C60 Bisadduct (ICBA) in Ternary Organic Solar Cells. *Energy Environ. Sci.* **2013**, *6* (6), 1796−1801.
(16) Lu, L.; Xu, T.; Chen, W.; Landry, E. S.; Yu, L. Ternary Blend Polymer Solar Cells with Enhanced Power Conversion Efficiency. *Nat. Photonics* **2014**, *8* (9), 716−722.
(17) Yang, Y.; Chen, W.; Dou, L.; Chang, W.-H.; Duan, H.-S.; Bob, B.; Li, G.; Yang, Y. High-Performance Multiple-Donor Bulk Heterojunction Solar Cells. *Nat. Photonics* **2015**, *9* (3), 190−198.
(18) Cheng, P.; Li, Y.; Zhan, X. Efficient Ternary Blend Polymer Solar Cells with Indene-C60 Bisadduct as an Electron-Cascade Acceptor. *Energy Environ. Sci.* **2014**, *7* (6), 2005−2011.
(19) Huang, T.-Y.; Patra, D.; Hsiao, Y.-S.; Chang, S. H.; Wu, C.-G.; Ho, K.-C.; Chu, C.-W. Efficient Ternary Bulk Heterojunction Solar Cells Based on Small Molecules Only. *J. Mater. Chem. A* **2015**, *3* (19), 10512−10518.

DOI: 10.1021/acsami.5b06831
ACS Appl. Mater. Interfaces 2015, 7, 22542−22550

(20) Ko, S.-J.; Lee, W.; Choi, H.; Walker, B.; Yum, S.; Kim, S.; Shin, T. J.; Woo, H. Y.; Kim, J. Y. Improved Performance in Polymer Solar Cells Using Mixed $PC_{61}BM/PC_{71}BM$ Acceptors. *Adv. Energy Mater.* **2015**, *5* (5), 1401687.
(21) Khlyabich, P. P.; Burkhart, B.; Thompson, B. C. Efficient Ternary Blend Bulk Heterojunction Solar Cells with Tunable Open-Circuit Voltage. *J. Am. Chem. Soc.* **2011**, *133* (37), 14534−14537.
(22) Cha, H.; Chung, D. S.; Bae, S. Y.; Lee, M.-J.; An, T. K.; Hwang, J.; Kim, K. H.; Kim, Y.-H.; Choi, D. H.; Park, C. E. Complementary Absorbing Star-Shaped Small Molecules for the Preparation of Ternary Cascade Energy Structures in Organic Photovoltaic Cells. *Adv. Funct. Mater.* **2013**, *23* (12), 1556−1565.
(23) Huang, J.-H.; Velusamy, M.; Ho, K.-C.; Lin, J.-T.; Chu, C.-W. A Ternary Cascade Structure Enhances the Efficiency of Polymer Solar Cells. *J. Mater. Chem.* **2010**, *20* (14), 2820−2825.
(24) Rousseau, T.; Cravino, A.; Bura, T.; Ulrich, G.; Ziessel, R.; Roncali, J. Multi-Donor Molecular Bulk Heterojunction Solar Cells: Improving Conversion Efficiency by Synergistic Dye Combinations. *J. Mater. Chem.* **2009**, *19* (16), 2298−2300.
(25) Khlyabich, P. P.; Burkhart, B.; Thompson, B. C. Compositional Dependence of the Open-Circuit Voltage in Ternary Blend Bulk Heterojunction Solar Cells Based on Two Donor Polymers. *J. Am. Chem. Soc.* **2012**, *134* (22), 9074−9077.
(26) Yang, L.; Zhou, H.; Price, S. C.; You, W. Parallel-Like Bulk Heterojunction Polymer Solar Cells. *J. Am. Chem. Soc.* **2012**, *134* (12), 5432−5435.
(27) Chang, S.-Y.; Liao, H.-C.; Shao, Y.-T.; Sung, Y.-M.; Hsu, S.-H.; Ho, C.-C.; Su, W.-F.; Chen, Y.-F. Enhancing the Efficiency of Low Bandgap Conducting Polymer Bulk Heterojunction Solar Cells Using P3HT as a Morphology Control Agent. *J. Mater. Chem. A* **2013**, *1* (7), 2447−2452.
(28) Ameri, T.; Khoram, P.; Heumuller, T.; Baran, D.; Machui, F.; Troeger, A.; Sgobba, V.; Guldi, D. M.; Halik, M.; Rathgeber, S.; Scherf, U.; Brabec, C. J. Morphology Analysis of Near IR Sensitized Polymer/Fullerene Organic Solar Cells by Implementing Low Bandgap Heteroanalogue C-/Si-PCPDTBT. *J. Mater. Chem. A* **2014**, *2* (45), 19461−19472.
(29) Jeong, S.; Kwon, Y.; Choi, B.-D.; Ade, H.; Han, Y. S. Improved Efficiency of Bulk Heterojunction Poly(3-hexylthiophene):[6,6]-phenyl-C61-butyric Acid Methyl Ester Photovoltaic Devices Using Discotic Liquid Crystal Additives. *Appl. Phys. Lett.* **2010**, *96* (18), 183305.
(30) Jeong, S.; Kwon, Y.; Choi, B.-D.; Kwak, G.; Han, Y. S. Effects of Nematic Liquid Crystal Additives on the Performance of Polymer Solar Cells. *Macromol. Chem. Phys.* **2010**, *211* (23), 2474−2479.
(31) Sharenko, A.; Treat, N. D.; Love, J. A.; Toney, M. F.; Stingelin, N.; Nguyen, T.-Q. Use of a Commercially Available Nucleating Agent to Control the Morphological Development of Solution-Processed Small Molecule Bulk Heterojunction Organic Solar Cells. *J. Mater. Chem. A* **2014**, *2* (38), 15717−15721.
(32) Zhang, Y.; Deng, D.; Lu, K.; Zhang, J.; Xia, B.; Zhao, Y.; Fang, J.; Wei, Z. Synergistic Effect of Polymer and Small Molecules for High-Performance Ternary Organic Solar Cells. *Adv. Mater.* **2015**, *27* (6), 1071−1076.
(33) Zhang, J.; Zhang, Y.; Fang, J.; Lu, K.; Wang, Z.; Ma, W.; Wei, Z. Conjugated Polymer-Small Molecule Alloy Leads to High Efficient Ternary Organic Solar Cells. *J. Am. Chem. Soc.* **2015**, *137* (25), 8176−8183.
(34) Patra, D.; Huang, T.-Y.; Chiang, C.-C.; Maturana, R. O. V.; Pao, C.-W.; Ho, K.-C.; Wei, K.-H.; Chu, C.-W. 2-Alkyl-5-thienyl-Substituted Benzo[1,2-b:4,5-b′]dithiophene-Based Donor Molecules for Solution-Processed Organic Solar Cells. *ACS Appl. Mater. Interfaces* **2013**, *5* (19), 9494−9500.
(35) Malliaras, G. G.; Salem, J. R.; Brock, P. J.; Scott, C. Electrical Characteristics and Eficiency of Single-Layer Organic Light-Emitting Diodes. *Phys. Rev. B: Condens. Matter Mater. Phys.* **1998**, *58* (20), R13411−R13414.
(36) Zerdan, R. B.; Shewmon, N. T.; Zhu, Y.; Mudrick, J. P.; Chesney, K. J.; Xue, J.; Castellano, R. K. The Influence of Solubilizing Chain Stereochemistry on Small Molecule Photovoltaics. *Adv. Funct. Mater.* **2014**, *24* (38), 5993−6004.
(37) Farahat, M. E.; Wei, H.-Y.; Ibrahem, M. A.; Boopathi, K. M.; Wei, K.-H.; Chu, C.-W. A Dual-Functional Additive Improves the Performance of Molecular Bulk Heterojunction Photovoltaic Cells. *RSC Adv.* **2014**, *4* (18), 9401−9411.
(38) Tamayo, A.; Kent, T.; Tantitiwat, M.; Dante, M. A.; Rogers, J.; Nguyen, T.-Q. Influence of Alkyl Substituents and Thermal Annealing on the Film Morphology and Performance of Solution Processed, Diketopyrrolopyrrole-Based Bulk Heterojunction Solar Cells. *Energy Environ. Sci.* **2009**, *2* (11), 1180−1186.
(39) Schlenker, C. W.; Barlier, V. S.; Chin, S. W.; Whited, M. T.; McAnally, R. E.; Forrest, S. R.; Thompson, M. E. Cascade Organic Solar Cells. *Chem. Mater.* **2011**, *23* (18), 4132−4140.
(40) Khlyabich, P. P.; Rudenko, A. E.; Street, R. A.; Thompson, B. C. Influence of Polymer Compatibility on the Open-Circuit Voltage in Ternary Blend Bulk Heterojunction Solar Cells. *ACS Appl. Mater. Interfaces* **2014**, *6* (13), 9913−9919.
(41) Peumans, P.; Uchida, S.; Forrest, S. R. Efficient Bulk Heterojunction Photovoltaic Cells Using Small-Molecular-Weight Organic Thin Films. *Nature* **2003**, *425* (6954), 158−162.
(42) Ma, W.; Yang, C.; Gong, X.; Lee, K.; Heeger, A. J. Thermally Stable, Efficient Polymer Solar Cells with Nanoscale Control of the Interpenetrating Network Morphology. *Adv. Funct. Mater.* **2005**, *15* (10), 1617−1622.
(43) Ameri, T.; Min, J.; Li, N.; Machui, F.; Baran, D.; Forster, M.; Schottler, K. J.; Dolfen, D.; Scherf, U.; Brabec, C. J. Performance Enhancement of the P3HT/PCBM Solar Cells through NIR Sensitization Using a Small-Bandgap Polymer. *Adv. Energy Mater.* **2012**, *2* (10), 1198−1202.
(44) Leong, W. L.; Welch, G. C.; Seifter, J.; Seo, J. H.; Bazan, G. C.; Heeger, A. J. Understanding the Role of Thermal Processing in High Performance Solution Processed Small Molecule Bulk Heterojunction Solar Cells. *Adv. Energy Mater.* **2013**, *3* (3), 356−363.
(45) Guan, Z.; Wu, R.; Zang, Y.; Yu, J. Small Molecule Dye Rubrene Doped Organic Bulk Heterojunction Solar Cells. *Thin Solid Films* **2013**, *539* (0), 278−283.
(46) Cho, Y. J.; Lee, J. Y.; Chin, B. D.; Forrest, S. R. Polymer Bulk Heterojunction Photovoltaics Employing a Squaraine Donor Additive. *Org. Electron.* **2013**, *14* (4), 1081−1085.
(47) Nismy, N. A.; Jayawardena, K. D. G. I.; Adikaari, A. A. D. T.; Silva, S. R. P. Photoluminescence Quenching in Carbon Nanotube-Polymer/Fullerene Films: Carbon Nanotubes as Exciton Dissociation Centres in Organic Photovoltaics. *Adv. Mater.* **2011**, *23* (33), 3796−3800.
(48) Lee, J.; Yun, M. H.; Kim, J.; Kim, J. Y.; Yang, C. Toward the Realization of A Practical Diketopyrrolopyrrole-Based Small Molecule for Improved Efficiency in Ternary BHJ Solar Cells. *Macromol. Rapid Commun.* **2012**, *33* (2), 140−145.
(49) Zhou, W.; Shi, J.; Lv, L.; Chen, L.; Chen, Y. A Mechanistic Investigation of Morphology Evolution in P3HT-PCBM Films Induced by Liquid Crystalline Molecules Under External Electric Field. *Phys. Chem. Chem. Phys.* **2015**, *17* (1), 387−397.
(50) Warren, B. E. X-Ray Diffraction in Random Layer Lattices. *Phys. Rev.* **1941**, *59* (9), 693−698.

DOI: 10.1021/acsami.5b06831
ACS Appl. Mater. Interfaces 2015, 7, 22542−22550